Implementation of AUV and Ship Noise for Link Quality Evaluation in the DESERT Underwater Framework

Emanuele Coccolo
DEI, University of Padova
Padova, Italy
coccoloe@dei.unipd.it

Filippo Campagnaro
DEI, University of Padova
Padova, Italy
campagn1@dei.unipd.it

Alberto Signori
DEI, University of Padova
Padova, Italy
signoria@dei.unipd.it

Federico Favaro
DEI, University of Padova
Padova, Italy
federico.favaro@dei.unipd.it

Michele Zorzi
DEI, University of Padova
Padova, Italy
zorzi@dei.unipd.it

ABSTRACT

The underwater acoustic channel exhibits many challenges for communications. Since the underwater environment is becoming crowded with both static and mobile users, additional noise is produced in the channel by the physical components of the nodes. In particular, the noise generated by vessels causes interference to the packets transmitted by the acoustic modems, with a consequent increase in packet loss. This paper proposes methods for the simulation of the additive noise introduced by vessels traveling near or inside the network area. Specifically, the simulations include the presence of an Autonomous Underwater Vehicle (AUV) and a cargo ship, distinguished by their own noise patterns, in an underwater acoustic sensors network. All simulations have been performed with the DESERT Underwater framework.

KEYWORDS

Underwater acoustic networks; acoustic noise modeling; DESERT Underwater; network simulations, multimodal acoustic networks.

1 INTRODUCTION

Generally, underwater assets include both static nodes and mobile nodes, such as Autonomous Underwater Vehicles (AUVs) and Remotely Operated Vehicles (ROVs) [1], that transmit and receive data through acoustic or optical signals. While low-frequency acoustic signals [2] are used for control and monitoring traffic in long range communications, high-frequency acoustic [3] or optical signals [4] are used for data transfer in short range communications [5, 6]. Underwater acoustic networks are subjected to several external factors, that weaken the communication quality between transmitting and receiving nodes. One of these factors, that has not been exhaustively studied yet, is the impact of vessel traffic inside or near the network deployment. Indeed, the crafts traveling in proximity of a given network introduce an additive noise[1] component to the *Signal-to-Noise Ratio* (SNR) evaluation of the links, since machineries, propellers and physical phenomena, such as cavitation, lead to emissions of acoustic vibrations. Moreover, these vibrations have a behavior similar to that of the acoustic signals generated for transmission, so they follow the same propagation model proposed for the underwater acoustic channel [7]. Traditionally, in the simulation of an acoustic channel, the level of vessel noise is specified by setting the `shipping` factor, which changes the noise magnitude linearly in the decibel domain [8]. This approach is used in most of the state-of-the-art underwater network simulators, like Aqua Net [9], UnetStack [10] SUNSet [11], and DESERT Underwater [12]. However, these simulators neither characterize the shipping effect of different cargo types, nor react to events, like a new ship arrival/departure. Ns3 [13] provides the capability to model noisy nodes in the electromagnetic field, but its underwater library (UAN [14]) does not include the possibility to simulate any noisy vessels moving along the network.

WUWNet'18, December 3–5, 2018, Shenzhen, China

ACM ISBN 978-1-4503-6193-4/18/12…$15.00
https://doi.org/10.1145/3291940.3291966

[1] In this paper we refer to noise as the interference created by external sources, such as vessels, not related to the communication system but still affecting it.

The DESERT Underwater Framework [12], based on the MIRACLE extensions [15] of the network simulator ns2, serves as an affordable and effective tool for underwater network simulations: in this paper, we propose a method to better simulate the influence of vessels on acoustic communication. With this auxiliary factor in the simulator, we can better model the behavior of networks that undergo vessel traffic with high probability, like those near coasts or near off-shore facilities.

In Section 2, we present a noise model for different crafts, based on their nature and building characteristics, and in Section 3 we describe how this model is introduced in the DESERT Underwater Framework. In Section 4, we propose a network scenario that contains both a ship and an AUV, and enables us to evaluate the effect that artificial noise has on different frequencies. In Section 5 we show the results obtained with the configuration explained in Section 4, evaluating benefits and disadvantages of using medium-frequency instead of low-frequency acoustic links in such a noisy environment. In Section 6 we finally draw our concluding remarks.

2 NOISE ANALYSIS AND MODELING

For modeling purposes, nodes should be distinguished by their mobility and, if mobile, by their type of propulsion. In our model, we will consider the noise caused by mobile nodes, making a further distinction between ships and AUVs, since building characteristics and type of engine are significantly different.

2.1 Noise caused by ships

The previous version of DESERT Underwater lacks an implemented model that can distinguish the vehicles with respect to their construction characteristics, such as propulsion type, draft, length, and year of construction.[2] Furthermore, another important aspect to take into account is the impact of traveling speed of the vehicle on the noise generation. The AQUO Project results [16] offer a ship noise analysis useful to satisfy these requirements. Essentially, the noise is decomposed into three major aspects: *machinery*, *propeller* and *cavitation*.

This distinction leads to a helpful model, which considers both the size of the vehicle and the traveling speed. Specifically, the *machinery* and *propeller* components of the noise directly depend on the building characteristics of the ship, and the cavitation appears only when the propeller reaches the *cavitation inception speed*. This phenomenon consists in the development of bubbles around the propeller blades, that, both when they are generated and when they collapse, radiate a specific signal pattern, that increases considerably the noise above 200 Hz. In particular, the frequency of higher cavitation noise shifts to lower frequencies, but still can impact those that are used for communications.

[2]Cargo boats built in the late '70s are more noisy than modern ships built after 2000 [16].

The patterns are identified by the *reference length* of the craft and by the *cavitation inception speed*, different for each type of vessel. Also, the ships considered for this model are large commercial vessels which include cargo ships, cruise ships and ferries.

Moreover, as shown in [16], the vessels have different technical specifications and the components, in general, operate at different frequencies. For example, the machinery noise is predominant at low frequencies, unlike the cavitation and propeller noise, so that the frequency domain can be divided in two different regions by a cutoff frequency, f_{mach}. In the first interval the noise is assumed flat, whereas in the second interval it decays by a factor K_2 per decade:

$$SD_{mach}(f, V) = K_1 + K_2 \log f + K_3 \log V \tag{1}$$

where K_i are the weighting coefficients for each type of vessel (some examples can be found in [16]), V is the velocity of the vessel, f is the frequency. Also the equations for propeller noise and cavitation noise, presented in (2), have a structure similar to Equation (1).

$$\begin{aligned} SD_{prop}(f, V) &= K_4 + K_5 \log f + K_6 \log V \\ SD_{cav}(f, V) &= K_7 + K_8 \log f + K_9 \log V. \end{aligned} \tag{2}$$

For example, we report in Equation (3) the formulas obtained in [16] for the noise of a cargo ship (length 180 m, with a cavitation inception speed of 10 kts), used as the noise source in all the simulations presented in this paper.

$$\begin{aligned} SD_{mach}(f, V) &= 186 - 22 \log f + 15 \log V \\ SD_{prop}(f, V) &= 156 - 30 \log f + 50 \log V \\ SD_{cav}(f, V) &= 129 - 20 \log f + 60 \log V. \end{aligned} \tag{3}$$

The total radiated noise is given by

$$\begin{aligned} SD_{TOT} = 10 \log \Bigg(& 10^{\frac{SD_{mach}(f,V)}{10}} + 10^{\frac{SD_{prop}(f,V)}{10}} \\ & + 10^{\frac{SD_{cav}(f,V)}{10}} \Bigg) + 25 \log \left(\frac{L}{L_{ref}} \right) \end{aligned} \tag{4}$$

where L is the length of the vessel and L_{ref} is the reference length equal to 180 m.

The provided models have a similar behavior to the Ross model [17] but, in addition, the formulas are weighted to the specific pattern obtained during sea trials, and they are directly dependent on the ship velocity.

In Fig. 1 we show the plot of Equation (4), using the model for a cargo whose formulas are given in Equation (3).

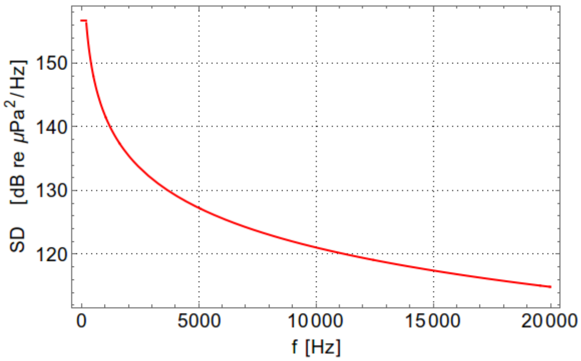

Figure 1: Noise power spectral density for a cargo ship of length 180 m, traveling at 15 knots of speed.

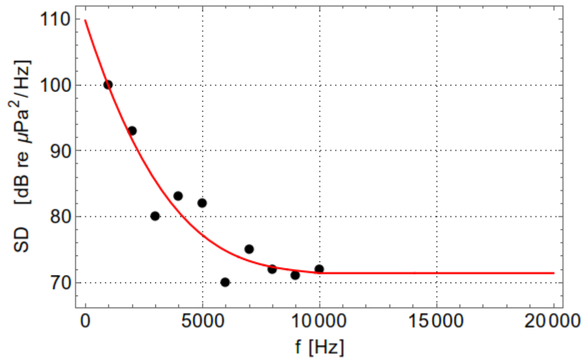

Figure 2: Model for noisy AUV, pre-modifications.

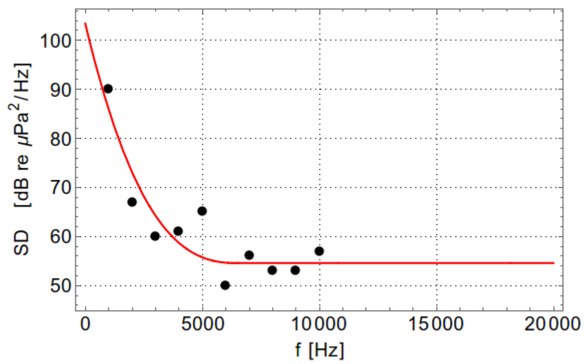

Figure 3: Model obtained for less noisy AUV, post-modifications.

2.2 Noise caused by AUV propellers

The AUV noise heavily differs from ship noise for both magnitude and components. Indeed, here the propeller velocity is much lower than in ships, thus the cavitation phenomenon does not appear in these devices. Moreover, the AUVs make use of electric power instead of diesel, so the vibrations of the hull are significantly lower.

There are no available models to represent the AUV noise so far, so we created a new one, starting from [18], which provides experimental results obtained with hydrophones mounted on the hull. This research offers two different settings for AUV noise: the first one is derived from an old AUV from Bluefin Robotics [19], the second one is the same AUV with slight custom modifications both in the propeller and in the gearbox, in order to decrease the emitted noise.

By fitting the retrieved data of both AUVs with polynomial curves, we obtain two models, depicted in Fig. 2 for the high noise AUV, and in Fig. 3 for the low noise AUV.

Only the noisier model has been inserted in the simulator, as the latter does not influence the acoustic link, since in this case the effect of the AUV can only be appreciated at small distances. The model for the noisy AUV is presented in Equation (5).

$$SD_{AUV} = \begin{cases} 10\log(113.392 - 0.01399f \\ \qquad +1.686 \cdot 10^{-6} f^2 & \text{for } f \leq 7982.5 \text{ Hz} \\ \qquad -7.119 \cdot 10^{-11} f^3), \\ 10\log(72.99) & \text{for } f > 7982.5 \text{ Hz} \end{cases} \tag{5}$$

3 VESSELS NOISE INCLUSION IN DESERT UNDERWATER

The effects of noise caused by external sources, such as AUVs or ships, have been included in the DESERT Underwater network simulator in two different ways. The former, presented in Section 3.1, includes the models presented in Section 2 in a new physical layer, called `uwphysicalnoise`. The latter, presented in Section 3.2, uses external lookup tables (LUTs) containing real field measurements of the additional external noise, without employing any mathematical model.

3.1 Ships and AUV noise model inclusion

Both the models described in Equation (4) and Equation (5) have been included in the SNR evaluation of a new physical module of the DESERT Underwater Framework, called `uwphysicalnoise`, in order to add the acoustic signal caused by the propellers to the existing background noise.[3] Specifically, we insert the list of the noisy nodes together with their position in the physical layer of each node of the network. This makes it possible to calculate the noise caused by ships and AUVs at the receiver, taking into account the propagation loss due to the distance between the noise sources and the receiving nodes, calculated at each packet reception.

Considering that the noise may be described by a generic function in the frequency domain, we need to numerically integrate the spectrum level given by the models over the

[3]Both the background noise and the channel model considered in this paper are presented in [8].

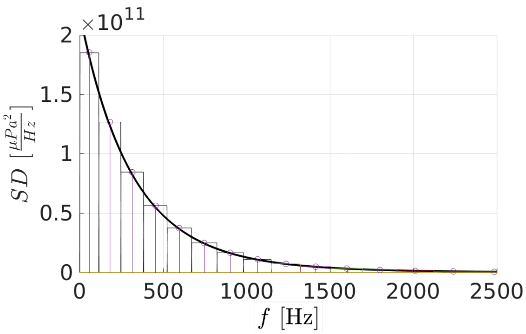

Figure 4: Noise slicing for AUV propellers, as reproduced from [18].

transmitting bandwidths. Since the integral is calculated every time a packet is received, we need to carefully select the parameters of the numerical integration, because there is a trade-off between computation time and precision of the results.

3.2 Additional noise inclusion as set of interfering packets

In order to be more general and let the user add the noise of a measured source, we present how to include in DESERT Underwater an external noise generator. In this model, the frequency spectrum is divided into sub-bands such that the noise can be considered constant in these frequency intervals. This is required due to the fact that noise has an exponential behavior in the frequency domain and, for the implementation proposed, we need to include in the simulator constant values. As a use case example, the division of the noise caused by the AUV propellers is depicted in Fig. 4, and included in DESERT in the form of a lookup table (LUT).

In order to include such acoustic source in DESERT Underwater, we considered the noise as a set of jamming signals operating in the spectral masks determined during the noise slicing process. Since the DESERT Underwater Framework is an event-based simulator, where the events are represented mostly by packets, the noise signal could be implemented as the transmission of subsequent packets, lasting for all the simulation time. In this way the artificial noise is considered at the physical layer as interference, and placed in the signal to noise and interference ratio (SINR), calculated as the ratio between the power of the signal containing the real packet, and the sum of the environmental noise and power of the interfering packets. In particular, in the list of interfering packets we consider both the actual interfering packets and the packets generated to simulate the artificial noise.

In order to make the noise signal last for all the simulation time, we can either use several subsequent small packets transmitted with a bitrate that lets them cover all the transmission period, or send just one long packet that lasts for all the simulated time. There are two major consequences in adopting these methods. First, the generation of dummy packets influences the execution time, since all these events are inserted in the scheduler and the transmission powers are included in the interference module of the physical stack in each node. Second, the node position at which the packet is transmitted is included in the header packet, thus, once the packet is sent, it contains statically the coordinates of the interfering node. This last aspect, in particular, demands that we make several considerations during the simulation modeling. Indeed, the solution with just one long packet imposes the interfering node to be static, since the positions are not upgraded and the noise power value is constant. A solution to this problem could be to dynamically adapt the length of the packets to the mobility pattern, i.e., sending shorter packets when the node is moving and longer packets when the node stops in a position for a long time.

In order to exploit such a model based on noise packets, a jammer module for the MAC layer was implemented, to let the noise generating node transmit regardless of the transmission policies used in the network. Indeed, such MAC layer discards all the packets received from the physical layer, and transmits either noise or jamming packets as soon as they are generated. The former packets are used for emulating continuous noise generated during a long period of time, while the latter are employed to simulate high power jamming packets lasting for a short period. To this aim, in the physical module, the noise packets are not sent up to the other layers, so that only the transmission power of these packets is taken into account in the interference module.[4] Otherwise, if the packets are intended to be generated for explicitly denying communications on the acoustic links (jamming packets), they are forwarded to the upper layers and discarded for different reasons than the nature of the packet, such as the wrong destination or wrong data type. Thus, the transmission of data packets can occur on top of other packets created for disturbance. In the case of AUV propellers noise, several packets are transmitted in parallel, at the power and the bandwidth given by the slicing presented in Figure 4.

4 SCENARIOS AND SIMULATION PARAMETERS

To better understand the influence of a craft traveling near or inside the network with respect to the spectrum used for transmission, we implemented two different networks, whose results lead to different insights.

Initially, we consider a simple network with just two nodes, described in Section 4.1, and then extend our analysis to a

[4] In this way all the DESERT MAC modules can be employed in the simulations without any change in the preexisting code.

more complicated case, presented in Section 4.2, with a network composed by 2 nodes equipped with medium frequency acoustic modems (MF), 2 nodes equipped with low frequency acoustic modems (LF), and one modem equipped with both MF and LF. All the simulations have been performed with the DESERT Underwater network simulator.

The noise injection was modeled with the mathematical evaluation for the ship noise, directly included in the SNR calculation at the reception of each packet (detailed in Section 3.1), and with long interfering dummy packets for the AUV noise (method presented in Section 3.2), since we consider the AUV to keep a fixed position in proximity of one of the nodes of the network.

We should note that the two scenarios have different purposes and their results should not be compared without considering the topologies. Indeed, the main differences between these networks are the number of transmitting nodes and the distances between nodes of different transmission modes (in scenario 2 the distances between LF nodes are twice the distances between MF nodes). This approach was driven by different goals: the first scenario was developed to study the two technologies in the same conditions (i.e., same transmission power and same distance); the second scenario, instead, outlines a generic multi-modal network where the technologies are employed for different reasons (long range communications for LF frequencies, short range communications for MF frequencies with higher bitrate available to the nodes).

4.1 Scenario 1: single acoustic link

In the first scenario we consider a simple network with just two nodes, communicating with a CSMA 1-persistent MAC protocol. Both nodes are equipped with both MF and LF: the parameters of carrier frequency and bandwidth are reported in Tab. 1. The transmitting parameters, that cover the PHY specifications, are picked following the characteristics of two acoustic modems available on the market: Develogic HAM.NODE [2] for LF and EvoLogics S2C 18/34 [20] for MF.

The two nodes are placed 3 km apart and deployed at the same depth of 100 m, while a cargo ship is initially placed at a distance of 200 m from Node 1 and 3 km from Node 2 and suddenly moves towards Node 2, with a constant speed that varies at each simulation run. The ship propeller (considered as a source of additional acoustic noise) is assumed to be placed at a depth of 5 m. Node 1 works as the sink of the network, as it collects data packets from Node 2. The network topology is depicted in Fig. 5.

With this configuration we can better understand the influence of an artificial craft on a single acoustic link, without worrying about different behaviors introduced by transmission and routing protocols. Of course, we expect a decay in the link quality as the ship approaches the sink.

Table 1: Summary of the simulation parameters

Parameter	Value
Sim duration	100000 s
LF carrier frequency	3.5 kHz
LF bandwidth	2 kHz
MF carrier frequency	23 kHz
MF bandwidth	16 kHz
TxPower	180 dB re μPa^2
Packet Size	125 byte (=10^3 bit)
Bitrate LF	1 kbit/s
Bitrate MF	4.8 kbit/s
Packet period	30 s

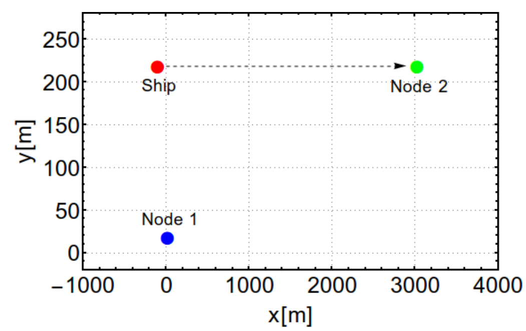

Figure 5: Scenario 1: network topology with two multimodal nodes. The dotted line is the path traveled by the ship.

Since the velocity of the cargo ship is a variable that affects the shipping noise, it can change significantly the link quality during transmission. For this reason, we made several simulations with different vessel speed values, to evaluate the effect of different configurations. The influence of the noise caused by a cargo ship on the performance of a single acoustic link is analyzed in Section 5.1.

4.2 Scenario 2: multimodal acoustic network

In the second scenario, we simulate a network with two sets of nodes that operate at different frequencies: the former set at LF, composed by Node 1, Node 2 and Node 3, with $f_{c,LF} = 3.5\ kHz$, and the latter at MF, composed by Node 3, Node 4 and Node 5, with $f_{c,MF} = 23\ kHz$. In each network, there are three nodes and, in particular, we model Node 3 as a multimodal node, which transmits at both low and high frequency, by placing two superimposed nodes. The topology of the network is shown in Fig. 6, where the multimodal node is placed in position $x = 2000$ m and $y = 2000$ m. Such node acts as a hub in a star topology: the routing table used in this network is presented in Table 2.

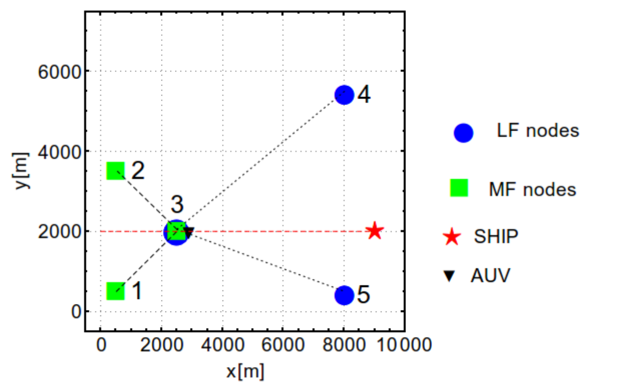

Figure 6: Scenario 2: topology of LF and MF networks. The dotted red line is the path traveled by the ship.

Table 2: Routing table for both LF and MF networks in scenario 2. *Node 3* is the hub in the star topology.

MF Network			LF Network		
Source	Dest.	Gateway	Source	Dest.	Gateway
1	2, 3	3	3	4	4
2	1, 3	3	3	5	5
3	1	1	4	3, 5	3
3	2	2	5	3, 4	3

In this scenario, a ship travels at a speed of 15 knots along a specific path (shown in Fig. 6 as a red dashed line), and passes over the hub node and then moves away from the network. The simulation period was shortened to 30000 seconds, so the vessel influences the transmissions of at least 2/3 of the simulation period (thus we can observe more clearly a decay with the insertion of artificial noise). Instead, in the first instance of this scenario the AUV is static and its propellers are placed at a distance of 1.5 meters from the hub node, as we want to simulate the hub node to be the AUV itself. In a second instance of this scenario, the AUV moves in the proximity of the hub node, this time assumed to be deployed from a fixed buoy, in order to inspect at which distance the AUV noise impairs the communication.

Table 3: TDMA parameters used in scenario 2

Parameter	LF	MF
Frame duration	21 s	15 s
Number of slots	3	3
Slot duration	7 s	5 s
Guard time	5.5 s	3 s

The MAC layer employed is TDMA: two different configurations (reported in Table 3) are employed for the LF and the MF networks and a guard time is placed between consecutive time slots in order to avoid packet collisions.

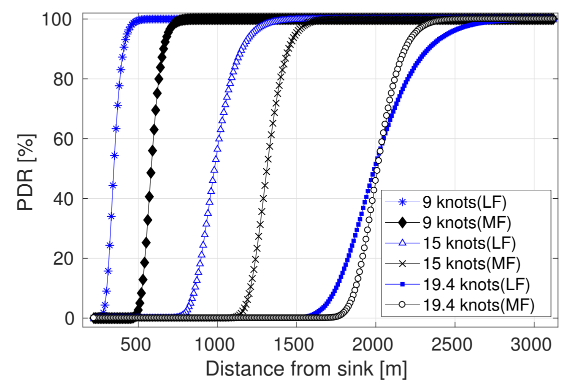

Figure 7: Packet Delivery Ratio with vessel traveling in the network shown in Fig. 5. The distance in the x-axis is referred to the distance between *Ship* and *Node 1* (sink).

5 RESULTS

In this section, we present the results of the simulations described in Section 4. In particular, in Section 5.1 we report how the ship velocity affects the noise in an acoustic link, while in Section 5.2 we discuss how the noise caused by an AUV and a cargo ship passing close to the nodes of the network influences the communications.

5.1 Influence of vessel speed in an acoustic communication

In Fig. 7 we present how a cargo vessel speed changes the shipping noise and, therefore, how it impairs the acoustic communication. In particular, we analyze the *Packet Delivery Ratio* (PDR), defined as the probability that a packet is received at the destination without errors, as a function of the distance between the noisy vessel and the sink (Node 1).

From the results, the speed turns out to be one of the most significant parameters that change the link quality between nodes. The velocities used in these simulations are 10 m/s (19.4 knots), 7.717 m/s (15 knots), and 4.63 m/s (9 knots). We highlight that 15 knots is, normally, the average traveling speed of a cargo vessel (type of craft used for this simulation), instead 9 knots is a speed just below the *cavitation inception speed*, so that in this case the cavitation noise component does not appear in the comprehensive formula for the radiated noise (Equation (4)).

Another important aspect is that, typically, the LF modems are used for long range communications at low rates, whereas the MF frequencies support a wider bandwidth, but are also

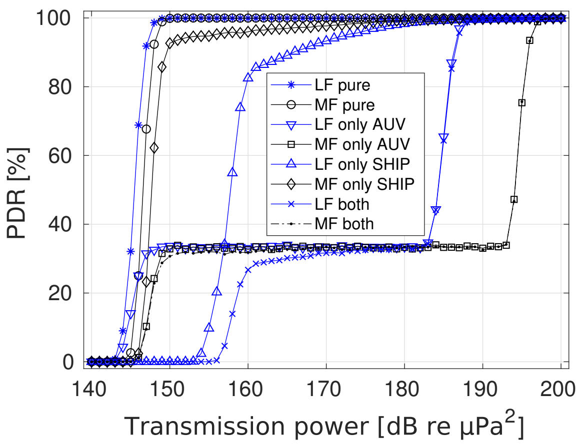

Figure 8: Results from the second scenario: PDR vs transmission power.

more subjected to absorption loss, due to the frequency-selective nature of the channel [8]. In this simulation, the nodes are close to the maximum range of the MF communications and less than half of the maximum range of the LF. For this reason in this scenario the MF has a higher decay than LF. We expect LF to have a behavior similar to MF if we place the node at a further distance.

5.2 Influence of shipping noise in a multimodal network

In Fig. 8 we present the overall PDR obtained in scenario 2 varying the transmission power of the nodes. The PDR has been obtained considering different sources of noise, for both LF and MF networks. The transmission power plays a key role in this study because it determines the level at which the nodes have to transmit to overcome the noise caused by the vessels. First, the simulations were run without the activation of the craft noise, to obtain a starting point from which the performance is expected to decay with the introduction of additional noise sources. In each simulation, the power was increased with an increment of 0.5 dB re μPa^2, and the results show that, at short range, the LF network can transmit more efficiently, in terms of energy spent, than the MF network. Actually, we see that an improvement in PDR is at a lower transmission power for the LF network (at least over 180 dB re μPa^2), but we have to consider that the two sub-networks have different distances, in particular longer between the LF nodes. With the introduction of external artificial noise, the performance of both networks drops. In particular, we can observe that LF reacts better than MF in the scenario with only AUV noise. Differently, with only ship noise, MF reacts better than LF. However, this scenario is also affected by the amount of time the nodes are exposed to the ship noise, that is bigger for LF than for MF.

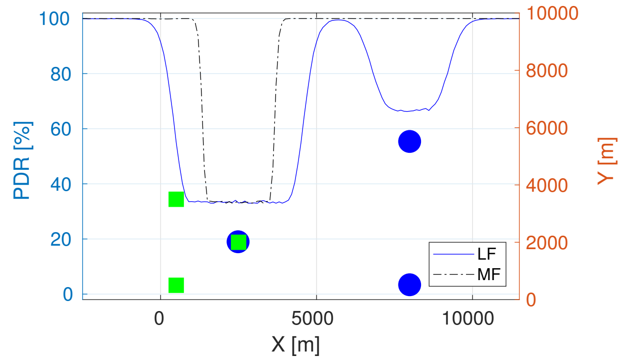

Figure 9: Overall packet delivery ratio when the ship is moving from x = -2500 m to x = 11500 m. The LF nodes are represented as blue circles and the MF nodes as green squares.

At first, it seems that the AUV noise has a higher impact on the reception of data packets, but we should consider that, in this configuration, the AUV is in close quarter for the entire simulation, thus it is expected to be the major cause of packet dropping for the links from the outer nodes.

In Fig. 9 we present the instantaneous behavior of the system when varying the ship position: in particular we plotted the instantaneous overall packet delivery ratio when the ship is moving from x = -2500 m to x = 11500 m with a traveling speed of 15 knots (7.717 m/s), when both LF and MF modems are transmitting with a power of 180 dB re μPa^2. In this figure the AUV noise is not considered.

When the ship is close to the hub, i.e., for $x = 2500$ m, the PDR goes down for both the LF and MF networks, because the noise generated by the ship decreases the link quality. In particular, most of the packets intended for the hub are not received correctly, and the PDR is close to 33%. Indeed, packets transmitted by Node 1 can be intended for either Node 2 or Node 3. When the destination is Node 3, the packets are not received correctly because of the ship noise. If the destination is Node 2, the packets are first transmitted to the hub (Node 3) to be then forwarded to Node 2, but these packets are lost in the first transmission from Node 1 to Node 3. Similarly for the packets transmitted by Node 2. Only the packets transmitted by Node 3 to Node 1 and Node 2 are received correctly, because they are not affected by ship noise. The behavior of the LF network is similar to the one just described for the MF network. When the ship moves farther away from the hub, the PDR increases because the noise power of the ship becomes lower. Between 4700 m and 7000 m we experience an increase in the link quality of the LF network. Indeed the ship is found in a position that does not interfere with the reception of packets, neither from the hub nor from the other LF nodes. As soon as the craft reaches the longitude of the satellite LF nodes, the performance of

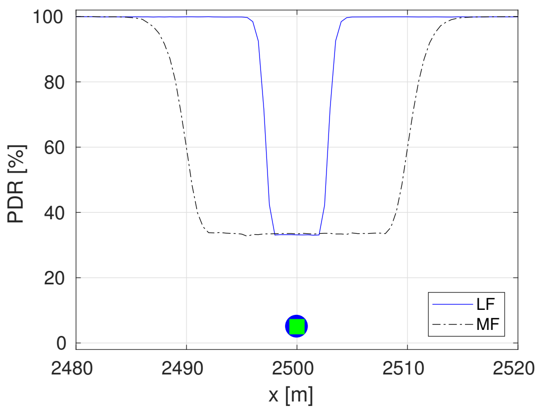

Figure 10: Overall packet delivery ratio when the AUV is moving from x = 2480 m to x = 2520 m.

the LF network decreases, since now the ship has shortened the distance enough to lower the SNR of those nodes.

Furthermore, we need to analyze the influence of AUV noise on the network without considering ship noise. Indeed, AUV noise power is lower than ship noise, so it starts to impair communications at a much lower distance, since the propagation affects even the noise signal. The results of the simulations, performed with the same procedure of Fig. 9, are given in Fig. 10, which presents a closer view on the x-axis. From the comparison between Figure 9 and Figure 10 we can observe how the ship noise affects more the LF communication, while the AUV noise the MF communication, confirming the trend presented in Figure 8.

6 CONCLUSIONS

In this paper we presented a way to simulate the injection of noise in an underwater network, working with the DESERT Underwater Framework. The noise was introduced through a lookup table, where each entry corresponds to a noise level for a specific carrier frequency for the AUV crafts, and via mathematical models for ship vessels. The ship models were obtained from the research of the AQUO Project; instead, for characterizing the AUVs, we used Zimmerman's data trials.

The results revealed that the lower frequencies react worse than the medium frequencies to the noise caused by a cargo ship, but better to the noise caused by an AUV. Further works will inspect how a multimodal network can be employed in this scenario to overcome the noise issue, by switching between LF and MF according to the surrounding noise sources. Other interesting items for future work include the enhancement of the noise representation as a set of interfering packets by adapting their length to the mobility pattern of the nodes, as well as the addition to the noise model of the mechanical noise which is generated by collisions or banging of metal parts, such as the banging between chainrings around the acoustic modem.

ACKNOWLEDGMENT

This work has has been developed with the support of WTD71, Underwater Communication department 630, Kiel, Germany.

REFERENCES

[1] A. Micallef *et al.*, *Submarine Geomorphology*. Springer, 2017.
[2] "Develogic Subsea Systems," Last time accessed: Sep. 2018. [Online]. Available: http://www.develogic.de/
[3] "Evologics S2C M HS modem," accessed: Sep. 2018. [Online]. Available: http://www.evologics.de/en/products/acoustics/s2cm_hs.html
[4] M. Doniec, A. Xu, and D. Rus, "Robust real-time underwater digital video streaming using optical communication," in *Proc. ICRA*, Karlsruhe, Germany, May 2013.
[5] F. Campagnaro, F. Guerra, F. Favaro, V. S. Calzado, P. Forero, M. Zorzi, and P. Casari, "Simulation of a multimodal wireless remote control system for underwater vehicles," in *Proc. ACM WUWNet*, Washington, DC, Oct. 2015.
[6] F. Campagnaro *et al.*, "Simulation of multimodal optical and acoustic communications in underwater networks," in *Proc. MTS/IEEE OCEANS*, Genova, Italy, May 2015.
[7] M. Stojanovic and J. Preisig, "Underwater acoustic communication channels: Propagation models and statistical characterization," *IEEE Communications Magazine*, vol. 47, no. 1, pp. 84–89, January 2009.
[8] M. Stojanovic, "On the relationship between capacity and distance in an underwater acoustic communication channel," *SIGMOBILE Mob. Comput. Commun. Rev.*, vol. 11, no. 4, pp. 34–43, Oct. 2007.
[9] Y. Zhu, S. Le, L. Pu, X. Lu, Z. Peng, and J. Cui, "Towards experimental evaluation of software-defined underwater networked systems," in *Proc. MTS/IEEE Oceans*, San Diego, CA, Sep. 2013.
[10] The NUS ARL and SubNero, "UNET–The Underwater NETworks project," Last time accessed: Sep. 2018. [Online]. Available: http://www.unetstack.net
[11] C. Petrioli, R. Petroccia, and D. Spaccini, "SUNSET version 2.0: Enhanced framework for simulation, emulation and real-life testing of underwater wireless sensor networks," in *Proc. ACM WUWNet*, Kaohsiung, Taiwan, Nov. 2013.
[12] F. Campagnaro *et al.*, "The DESERT underwater framework v2: Improved capabilities and extension tools," in *Proc. Ucomms*, Lerici, Italy, Sep. 2016.
[13] ns3 Network Simulator, http://www.isi.edu/nsnam/ns/, Last time accessed: Sep. 2018.
[14] "UAN framework," accessed: Sep. 2018. [Online]. Available: https://www.nsnam.org/docs/release/3.12/models/html/uan.html
[15] N. Baldo, M. Miozzo, F. Guerra, M. Rossi, and M. Zorzi, "Miracle: the multi-interface cross-layer extension of ns2," *EURASIP J. of Wireless Commun. and Networking*, 2010. [Online]. Available: http://www.hindawi.com/journals/wcn/aip.761792.html
[16] C. Audoly and E. Rizzuto, "Ship underwater radiated noise patterns," AQUO Project Consortium, final report R2.9, 06 2015.
[17] D. Ross, *Mechanics of Underwater Noise*. Los Altos, CA: Peninsula Publishing, 1987.
[18] R. Zimmerman, G. L. D'Spain, and C. D. Chadwell, "Decreasing the radiated acoustic and vibration noise of a mid-size AUV," *IEEE Journal of Oceanic Engineering*, vol. 30, no. 1, pp. 179–187, Jan 2005.
[19] GENERAL DYNAMICS, "Bluefin sandshark," last time accessed Sep. 2018. [Online]. Available: https://gdmissionsystems.com/bluefinrobotics/vehicles-batteries-and-services/bluefin-sandshark
[20] "S2CR 18/34 Acoustic Modem," Last time accessed: Sep. 2018. [Online]. Available: http://www.evologics.de/en/products/acoustics/s2cr_18_34.html/